JOURNAL OF OPTOELECTRONICS AND ADVANCED MATERIALS Vol. 12, No. 12, December 2010, p. 2355 - 2362

A simple method of fabricating efficient blue organic light-emitting diodes based on a double-dopant and a double-emissive layer with an effective hole-trapping architecture

H.-P. LIN[a*], X.-W. ZHANG[c], D.-B. YU[a], J. LI[a], L. ZHANG[a], F. ZHOU[a], X.-Y. JIANG[a,b], Z.-L. ZHANG[a, b]
[a]*Department of Materials Science, Shanghai University, Jiading, Shanghai 201800, People's Republic of China*
[b]*Key Laboratory of Advanced Display and System Applications, Ministry of Education, Shanghai University, Shanghai 200072, People's Republic of China*
[c]*Guangxi Key Laboratory of Information Materials, Guilin University of Electronic Technology, Guilin 541004, People's Republic of China.*

This paper presents blue organic light-emitting diodes (BOLEDs) based on double-dopant and double-emissive layer (EML) structures. We first fabricated single-EML BOLEDs based on a double-dopant system: a blue fluorescent host of 4,40-bis(2,2-diphenylvinyl)-1,10-biphenyl (DPVBi) doped with a blue dopant of 1,4-bis[2-(3-N-ethylcarbazoryl)vinyl]benzene (BCzVB) and an assistant dopant of 2,3,6,7-tetrahydro-1,1,7,7,-tetramethyl-1H,5H,11H-10(2-benzothiazolyl) quinolizine-[9,9a,1gh]coumarin (C545T). Furthermore, we fabricated double-EML BOLEDs following the double-dopant structure: DPVBi doped with BCzVB is used as blue emitter, and this blue matrix doped with C545T is used as bluish-green emitter. The double-EML devices show a striking improvement in chromaticity and current efficiency as compared to the corresponding single-EML counterpart. This could be explained by the fact that the DPVBi layer impedes hole injection at the interface which greatly enhances the recombination of electron-hole pairs and hence improves the carriers balance in the emission region.

(Received October 27, 2010; accepted November 25, 2010)

Keywords: Blue OLED, Double-dopant, Double-emissive layer, High current efficiency, Chromaticity, Energy transfer.

1. Introduction

Organic light-emitting diodes (OLEDs) have attracted much attention due to their potential applications in flat-panel displays since the pioneer work of Tang and VanSlyke [1]. In flat-panel display applications a full-color capability is required, especially white; the applications include not only backlight sources of liquid crystal displays (LCDs), but also candidates for next generation lightings [2, 3]. For color displays, a blue emitter with high efficiency and color saturation has to be adopted in white OLEDs (WOLEDs) to realize pure white emission. Although a large number of valuable red and green emitters that satisfy the requirements for WOLEDs have been flourished, excellent blue emitters are still rare and have been subject of considerable interest [4-11]. A variety of designs have been proposed to make blue OLEDs (BOLEDs), including multilayered structure consisting of two or more emissive layers (EML) [4, 5], using the doping technique to take an appropriate amount of dopant in the same EML [6, 7], making use of the exciplex formation based on which the blue light yields [8 , 9], and using the microcavity effect [10, 11]. Among these strategies, multilayered structure is especially important in developing OLEDs. This is because the multilayered devices show higher efficiency in companion with the single-EML counterparts [4, 5, 12-14]. However, the fabrication of high performance BOLEDs is still difficult due to the intrinsic low efficiency of blue materials. The precise control of dopants, the demand for an appropriate stacking sequence and thickness of EMLs are all important factors to improve the efficiency and chromaticity.

Doping system, which is composed of host and dopant materials, is usually utilized to obtain emission. When a host is doped with a small amount of dopants, it has been proposed to trigger a cascade energy transfer process. It well knows that 4, 40-bis (2, 2-diphenylvinyl)-1, 10-biphenyl (DPVBi) is used as a blue fluorescent host and 1, 4-bis [2-(3-N-ethylcarbazoryl) vinyl] benzene (BCzVB) as a blue dopant. In many studies, 2,3,6,7-tetrahydro-1,1,7,7,-tetramethyl-1H,5H,11H-10(2-benzothiazolyl)quinolizine-[9,9a,1gh]coumarin (C545T), which is well known for high fluorescent efficiency, is widely used as an assistant dopant for obtaining green, red and white emission [15-17]. To the best of our knowledge, few report on the C545T used in OLEDs for obtaining blue emission has been presented so far.

In this paper, we proposed BOLEDs based on double-dopant and double-EML structures. We first fabricated single-EML BOLEDs based on the

double-dopant system. A blue fluorescent host of DPVBi doped with a blue guest of BCzVB and an assistant dopant of C545T as the EML. Using this double-dopant, the double-dopant BOLEDs shows higher current efficiency as compared to the device without the dopant of C545T. The enhancement of efficiency could readily be realized with an appropriate selection of a matching dopant for efficient energy transfer. Furthermore, we fabricated double-EML BOLEDs based on the double-doped structure. The blue host of DPVBi doped with BCzVB is used as a blue emitter, and this blue matrix doped with C545T is used as a bluish-green emitter. Since DPVBi possesses a deep highest occupied molecular orbital (HOMO) level of 5.9 eV [18]. It is expected to behave as an effective trapping site for holes. We have observed that the double-EML BOLEDs show a striking improvement in chromaticity and current efficiency as compared to the corresponding single-EML counterpart. This could be explained by the fact that the first EML of DPVBi impedes hole injection at the interface which greatly enhances the recombination of electron-hole pairs and hence improves the carriers balance within the emission region.

2. Experimental details

In order to improve the performance of BOLEDs, we use the double-dopant and double-EML structures to construct a series of novel devices. Three kinds of devices have been fabricated and their properties are analyzed in detail. The BOLEDs were fabricated on indium tin oxide (ITO) coated glass substrate with a sheet resistance of 20 Ω/□. After routine chemical cleaning, the ITO was further treated by UV ozone for 600 seconds. The organic layers and cathode were thermally deposited at 1.0×10^{-4} Pa. The typical device structure was ITO / MoO_x / NPB / EML / BPhen / LiF / Al. Where *N, N*'-di (naphthalene-1-y1)-*N, N*'-dipheyl-benzidine (NPB) was used as a hole-transport layer and 4-7-diphenyl-1, 10-phenanlhroline (BPhen) as an electron-transport layer, LiF and Al were used as an electron-injection layer and cathode, respectively. The schematic structure of devices and chemical materials employed are shown in Fig. 1. The thickness of the deposited materials was monitored by using a quartz-crystal monitor. The deposition rate was ~0.5 nm/s for organic layers and ~2.5 nm/s for Al metal cathode.

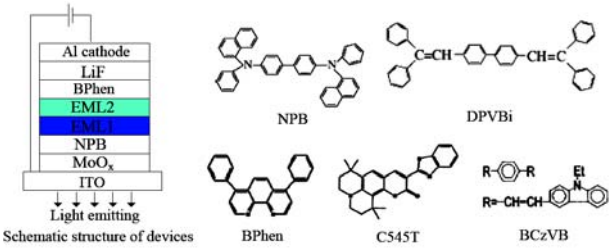

Fig. 1 The configuration of devices and molecular structures of main organics.

The active area of the devices was 2.5×10^{-5} m^2. The electroluminescent (EL) spectra and the Commission Internationale de L'Eclairage (CIE) color coordinates were measured by a PR-650 Spectra Scan. The current–voltage–luminance (I-V-L) measurements were performed using a Keithley 2400 Source Meter and a Minolta LS-110 Luminance Meter. The photoluminescent (PL) spectra and the optical absorption (Abs) spectra were taken with a Hitachi 850 Fluorescence Spectrophotometer.

3. Results and discussion

3.1. BOLEDs with double-dopant structure

We first fabricated single-EML BOLEDs based on a double-doped system. The devices having various doping concentration (from 0.025 to 0.80 wt %) were constructed as follows:

Type-A: ITO / MoO_x (4 nm) / NPB (30 nm) / [DPVBi: 5 % BCzVB: x % C545T] (20 nm) / BPhen (14 nm) / LiF (1 nm) / Al (120 nm) (x=0, device A0; x=0.025, device A1; x= 0.050, device A2; x= 0.075, device A3; x= 0.10, device A4; x= 0.20, device A5; x= 0.30, device A6; x= 0.40, device A7; x= 0.80, device A8)

Here, device A0 and device A1-A8 are the single-doped and double-doped devices, respectively. DPVBi, BCzVB, C545T are blue host, blue dopant and assistant dopant, respectively. Fig. 2 shows the EL spectra of these devices with different doping concentrations of C545T. It notes that the blue emission from the blue matrix of DPVBi at 460 nm matches a green emission from C545T at 496 nm, resulting in blue-green emission. The blue emission is observed to decrease with the increase of C545T doping, while the green emission increases. In all the devices, the broad EL spectra cover almost the entire visible region and the EL performances depend strongly on the concentration of C545T. In the case of lower C545T doping (from 0 to 0.30 wt %), the emission from DPVBi has been found stronger accordingly compared to that from C545T, resulting in blue emission. Meanwhile for the higher concentration of C545T (from 0.40 to 0.80 wt %), the emission from DPVBi is not as strong as the C545T emission, resulting in bluish-green emission.

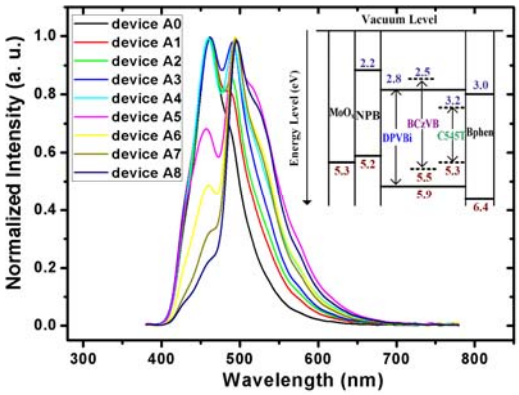

Fig. 2. Normalized EL spectra of Type-A devices at the current density of 20 mA/cm^2. The inset shows the energy diagram of the double-doped BOLEDs.

Fig. 3 shows the PL and the Abs spectra of deposited films of DPVBi, BCzVB, and C545T. It can be seen that there is a little overlap between the PL spectrum of DPVBi and Abs spectrum of C545T. In the case of BCzVB, the PL spectrum of DPVBi and the Abs spectrum of BCzVB well overlap. Furthermore, the PL of BCzVB is well covered the Abs of C545T. When the concentration of C545T was adjusted very small, a cascade energy transfer from DPVBi though BCzVB to C545T can occur. It indicates that the blue dopant of BCzVB works as a medium, leading to an efficient emission of C545T.

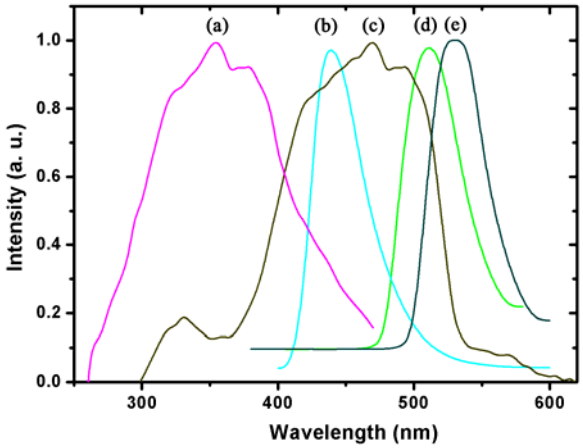

Fig. 3. (a) Abs of BCzVB (b) PL of DPVBi (c) Abs of C545T (d) PL of BCzVB and (e) PL of C545T.

Fig. 4 (a) and (b) show the current density-voltage and luminance-voltage (I-V-L) characteristics of Type-A devices. It can be seen that the double-doped devices (device A1-A6) show lower voltage than the single-doped device (device A0). For instance, as can be seen from Table 1, the driving voltage of device A0 is 9.6 V (20 mA/cm^2), while the devices A1-A6 have lower voltages of 7.4, 7.9, 8.2, 8.6, 8.7 and 9.3 V, respectively. However, when the concentration of C545T increases to 0.40 wt %, the driving voltage of devices A7 and A8 exceeds that of device A0. This trend indicates that the increase in C545T doping is responsible for the sharp change in carrier mobility, and thereby yields higher driving voltage. Our result is similar to the previous reported one [19], in which the concentration of C545T was deduced to play an important role in the carrier mobility. On the other hand, at the same driving voltage, the device with a lower C545T doping concentration shows a higher luminance. This could be in relation to its high carrier mobility, which facilitates energy transfer from the host of DPVBi to the dopant of C545T.

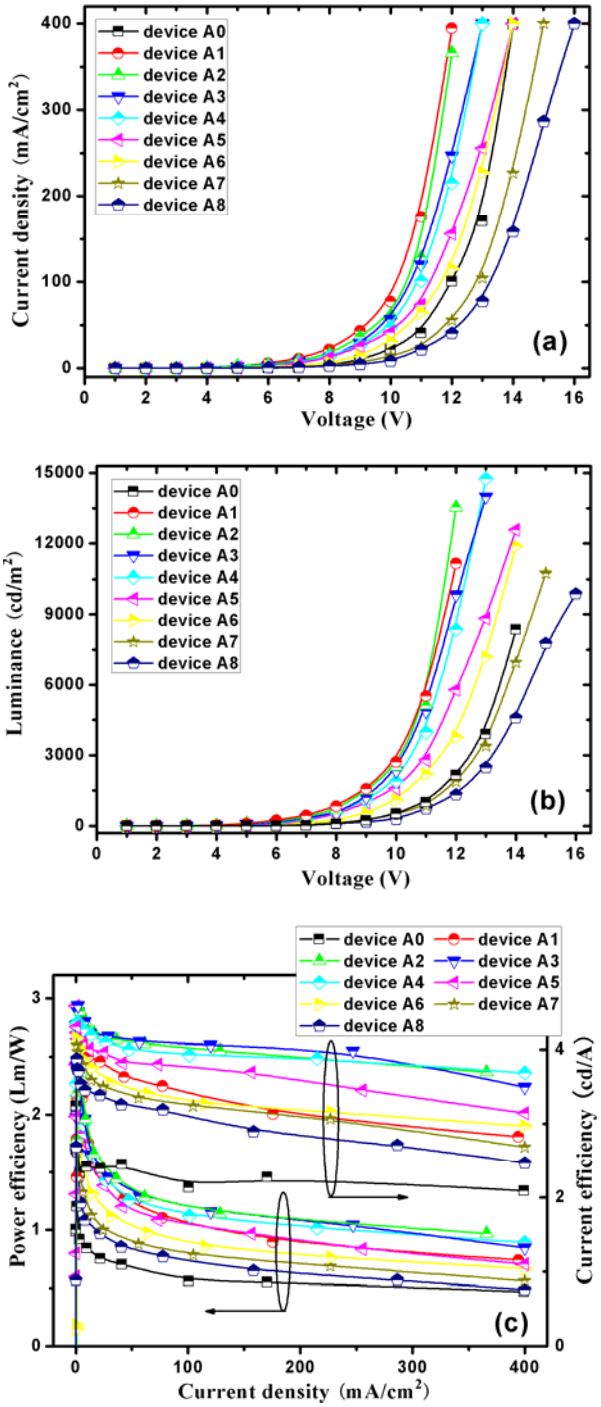

Fig. 4. (a) Voltage–current density (b) luminance–voltage and (c) EL efficiency–current density curves of Type-A devices.

Table 1. Characteristics of Type-A devices. C545T, L, V, η_L, η_p and CIE (x, y) were the C545T doping concentration, luminance, driving voltage, current efficiency, power efficiency and CIE color coordinates were at 20 mA/cm^2, respectively; the values inside the brackets were the maximum.

Devices	C545T (wt %)	L (cd/m^2)	V (V)	η_L (cd/A)	η_p (Lm/W)	CIE (x, y)
Device A0	0	497 (08 354,14[a])	9.6	2.40 (3.24)	0.79 (1.70)	(0.149, 0.155)
Device A1	0.025	632 (11 147,12[a])	7.4	3.86 (4.13)	1.73 (2.59)	(0.161, 0.213)
Device A2	0.050	493 (13 566,12[a])	7.9	4.27 (4.51)	1.95 (2.64)	(0.170, 0.225)
Device A3 [b]	**0.075**	**594 (13 987,13[a])**	**8.2**	**4.18 (4.64)**	**1.57 (2.88)**	**(0.166, 0.242)**
Device A4	0.10	711 (14 753,13[a])	8.6	4.02 (4.30)	1.51 (2.53)	(0.189, 0.271)
Device A5	0.20	827 (12 586,14[a])	8.7	3.98 (4.24)	1.42 (2.67)	(0.201, 0.342)
Device A6	0.30	879 (11 833,14[a])	9.3	3.63 (4.03)	1.26 (2.48)	(0.198, 0.369)
Device A7	0.40	742 (10 647,15[a])	10.1	3.50 (4.12)	1.03 (2.16)	(0.199, 0.422)
Device A8	0.80	529 (09 873,15[a])	10.8	3.41 (3.76)	0.98 (1.93)	(0.223, 0.481)

Note:

[a] the driving voltage corresponding to the maximum brightness.
[b] the most efficient single-EML device based on a double-dopant system.

The current and power efficiencies are shown in Fig. 4 (c). It is interesting to note that the double-doped BOLEDs show much better current efficiency and power efficiency than the single-doped device. For instance, device A3 shows the highest current efficiency of 4.64 cd/A and power efficiency of 2.88 Lm/W among these devices, while device A0 exhibits poor current efficiency of 2.34 cd/A and power efficiency of 1.70 Lm/W, respectively. Using this double-dopant system, the green component is greatly enhanced due to the increasing number of C545T molecules across the interfacial regions. It results in the enhancement of green component as well as the device efficiency. In addition, the improved efficiency in double-doped BOLEDs can be evidenced from the energy levels diagram (The inset of Fig. 2). It is clear that the HOMO level of BCzVB (5.5 eV) located between those of DPVBi (5.9 eV) and C545T (5.3 eV). The cascade energy transfer can explain the fact that the efficiency of double-doped devices is significantly improved.

3.2. Two-emitters BOLEDs with improved performance

In order to further improve the performance, we fabricated double-EML BOLEDs following the double-doped structure. A blue fluorescent host of DPVBi doped with BCzVB is used as a blue emitter (EML1), and this blue matrix doped with C545T is used as a bluish-green emitter (EML2). We adjusted the doping concentration of C545T at a certain sequence of the two emitters to achieve an appropriate fraction for emission. The configurations include,

Type-B: ITO / MoO_x (4 nm) / NPB (30 nm) / DPVBi: 5 % BCzVB (10 nm) / [DPVBi: 5 % BCzVB: y % C545T] (10 nm) / BPhen (14 nm) / LiF (1 nm) / Al (120 nm) (y=0.025, device B1; y= 0.050, device B2; y= 0.075, device B3; y= 0.10, device B4; y= 0.20, device B5; y= 0.30, device B6; y= 0.40, device B7; y= 0.80, device B8)

The EL spectra of Type-B devices are shown in Fig.5. The EL emission around 460 and 496 nm are from DPVBi and C545T, respectively. Since we fixed the weight ratio of blue matrix and C545T to unity, the EL intensities have been found comparable between the Type-A and Type-B devices. In this study, however, when a DPVBi layer doped with BCzVB is sandwiched between the NPB and EML2 layers, the emission from C545T is greatly reduced as compared with the corresponding single-EML counterpart. For example, at the current density of 20 mA/cm^2, the CIE color coordinates are (0.223, 0.481) and (0.184, 0.385) for devices A8 and B8, respectively.

This improvement in chromaticity can be attributed to the suppression of the C545T emission within emission region. Since the mobility of holes is higher by orders of magnitude than that of electrons. Moreover, holes are dominant in most OLEDs. The spectra change can be attributed to the hole-trapping behavior. According to the energy level diagram of the Type-B devices (see in the inset of Fig.5), the HOMO level of DPVBi is 5.9 eV, which is much higher than that of NPB (5.2 eV). It is well expected to act as an effective trapping site for holes. In our devices using a double-EML structure, injected holes from the anode into the first EML (EML1), recombine with injected electrons from the cathode and produce blue emission (from DPVBi and BCzVB). The extra holes further travel into the second EML (EML2) and again recombine with electrons, resulting in bluish-green emission (from the blue matrix and C545T). When the double-EML is used, the EML1 of DPVBi can greatly impede holes to enter the EML2. The blocked hole injection results in a smaller amount of holes available travel into the EML2 and recombine with electrons, which is reflected in the suppression of the C545T emission. Because in this case, the [DPVBi: BCzVB] matrix, to a certain extent, is working as a hole blocking layer.

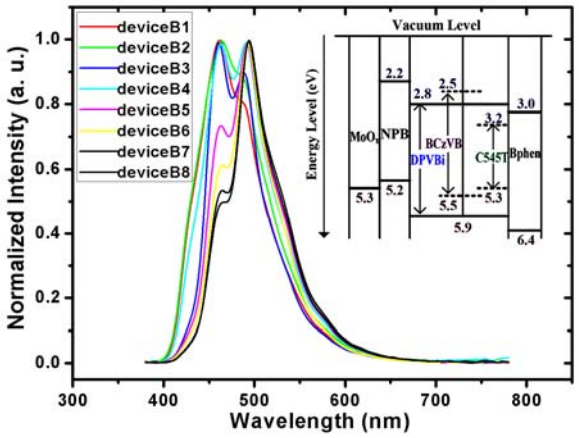

Fig. 5. Normalized EL spectra of Type-B devices at the current density of 20 mA/cm^2. The inset shows the energy diagram of the BOLEDs with a double-EML composed of EML1/EML2.

The I–V–L characteristics of Type-B devices are shown in Fig. 6 (a) and (b). It reveals that under the same current density the double-EML BOLEDs (see in Table 2) exhibit a bit higher driving voltages than do the single-EML devices. Indeed, the higher voltage of double-EML devices also supports this hole-trapping behavior, which is due to the increase in barrier height for hole-injection. In addition, the double-EML BOLEDs show much higher luminance in comparison with the single-EML counterparts.

Fig. 6 (c) gives the dependences of current and power efficiencies on the current density. It can be seen that double-EML devices show higher current and power efficiencies. For instance, device B2 reaches a current efficiency of 6.31 cd/A, which is 36 % and 95 % higher than that of device A3 and device A0, respectively. Its maximum power efficiency is 3.22 Lm/W, which is 1.12 times and 1.89 times than that of device A3 and device A0, respectively. These phenomena clearly indicate that the double-EML can significantly improve the EL efficiency.

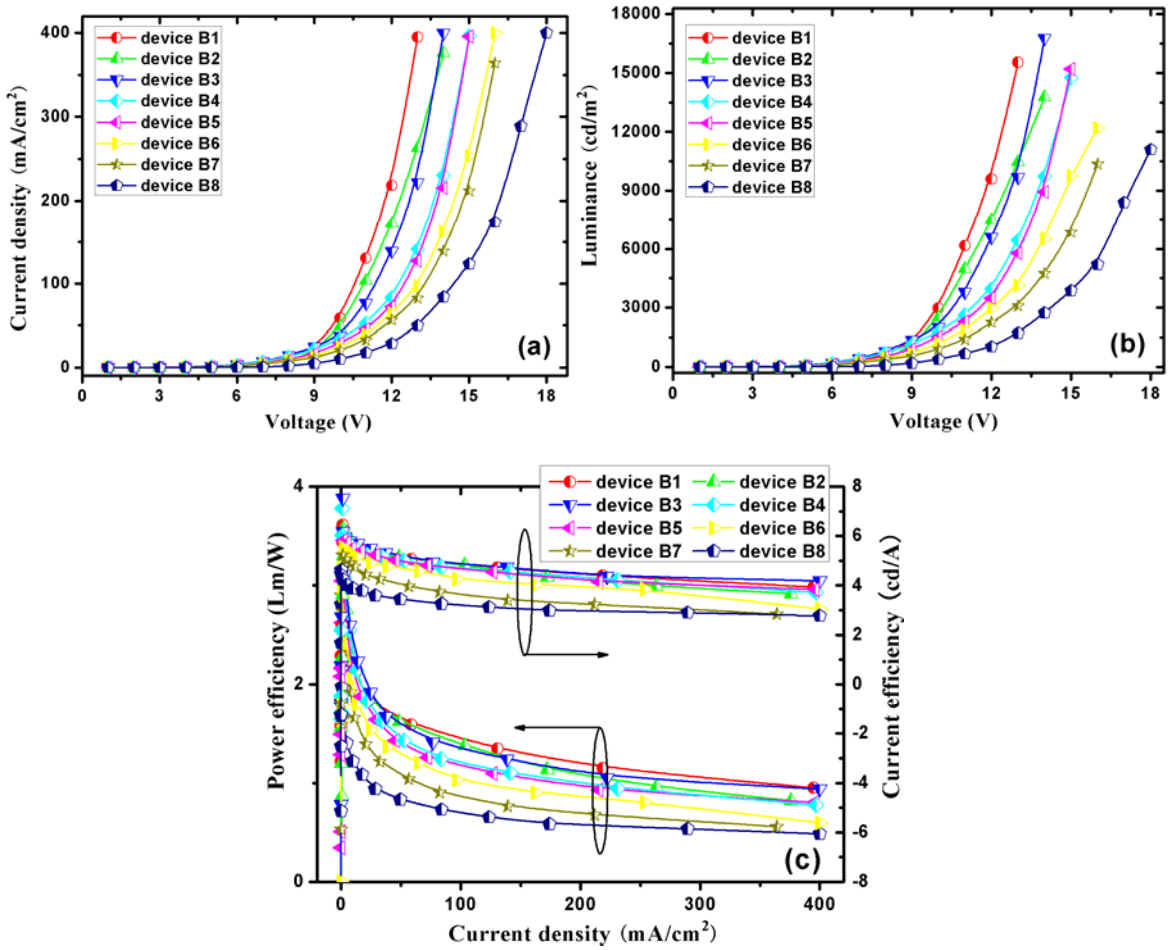

Fig. 6. (a) Voltage–current density (b) luminance–voltage and (c) EL efficiency–current density curves of Type-B devices.

Table 2. Characteristics of Type-B devices. C545T, L, V, η_L, η_p and CIE (x, y) were the C545T doping concentration, luminance, driving voltage, current efficiency, power efficiency and CIE color coordinates were at 20 mA/cm^2, respectively; the values inside the brackets were the maximum.

Devices	C545T (wt %)	L (cd/m^2)	V (V)	η_L (cd/A)	η_p (Lm/W)	CIE (x, y)
Device B1	0.025	851 (15 541,13[a])	8.3	5.32 (5.67)	2.05 (3.02)	(0.154, 0.198)
Device B2[b]	**0.050**	**957 (13 765,14[a])**	**8.5**	**5.46 (6.31)**	**1.97 (3.22)**	**(0.155, 0.212)**
Device B3	0.075	1 620(16 861,14[a])	9.2	5.39 (6.12)	1.85 (3.87)	(0.158, 0.231)
Device B4	0.10	1 386(14 659,15[a])	9.4	5.18 (6.01)	1.76 (3.14)	(0.161, 0.245)
Device B5	0.20	1 225(15 202,15[a])	9.8	5.27 (5.96)	1.78 (2.85)	(0.166, 0.316)
Device B6	0.30	1 543(12 190,16[a])	10.1	4.89 (5.49)	1.47 (2.52)	(0.164, 0.332)
Device B7	0.40	1 175(10 358,16[a])	10.4	4.31 (5.04)	1.31 (2.28)	(0.179, 0.379)
Device B8	0.80	867 (11 103,18[a])	11.3	3.72 (4.43)	0.95 (2.09)	(0.184, 0.385)

Note:

[a] the driving voltage corresponding to the maximum brightness.

[b] the most efficient double-EML device based on a double-dopant system.

In Type-B devices, there are four factors for the enhancement of current efficiency. First, a more balanced carriers are achieved by effectively blocking injected holes into emission region. The excess of hole injection in Type-A devices results in an unbalance of electrons and holes, which leads to a lower current efficiency. While hole injection of Type-B devices is much smaller than that of Type-A devices, the excess of holes logically decrease. Thus, the balance of electrons and holes is improved. Second, this hole-trapping property leads to an efficient recombination of electron-hole pairs in emission region. The accumulation of trapped holes helps establish a stronger electric field for enhancing electron injection, which also leads to a higher current efficiency. Third, C545T is used as an assistant dopant with high fluorescent efficiency, which can substantially enhance contribution from the broadband green emission. Last, the cascade energy transfer mechanism is taken place in the EL process. Overall, all these factors contribute to better balance of the carrier transport for both holes and electrons and thus the efficiency enhancement.

3.3. Two-emitters BOLEDs using different architecture

Although the BOLEDs have been successfully obtained, some other factors such as stacking sequence also contribute to the performance. For comparison, the devices with an opposite sequence of EML2/EML1 were also fabricated.

Type-C: ITO / MoO_x (4 nm) / NPB (30 nm) / [DPVBi: 5 % BCzVB: z % C545T] (10 nm) / DPVBi: 5 % BCzVB (10 nm) / BPhen (14 nm) / LiF (1 nm) / Al (120 nm) (z=0.025, device C1; z= 0.050, device C2; z= 0.075, device C3; z= 0.10, device C4; z= 0.20, device C5; z= 0.30, device C6; z= 0.40, device C7; z= 0.80, device C8)

Fig. 7 shows the EL spectra of the double-EML BOLEDs with a different sequence of EML2/EML1. In Type-C devices, the emission from C545T is rather strong (see in Table 3). For example, at the current density of 20 mA/cm^2, the CIE color coordinates are (0.198, 0.369), (0.164, 0.332) and (0.223, 0.482) for devices A6, B6 and C6, respectively. According to the energy level diagram (see in the inset of Fig.7), the dopant of C545T (5.3 eV) has a shallow HOMO level compared with the blue matrix of DPVBi (5.9 eV). Holes could easily enter into C545T, because the HOMO level of C545T is shallow compared to that of NPB (5.2 eV). In this case, more trapped carriers may form on C545T molecules and energy transfer from DPVBi to C545T more effectively. It leads to the increase of the green emission relative to the blue emission due to more electron and hole recombination at the interfaces during the photoexcitation. The change of the EL spectra can be evidenced by investigating the effect of the stacking sequence on the hole-trapping function in our devices. However, the CIE color coordinates remain unchanged as the doping concentration of C545T increases from 0.30 to 0.80 wt %. This means that the concentration quenching of C545T happens.

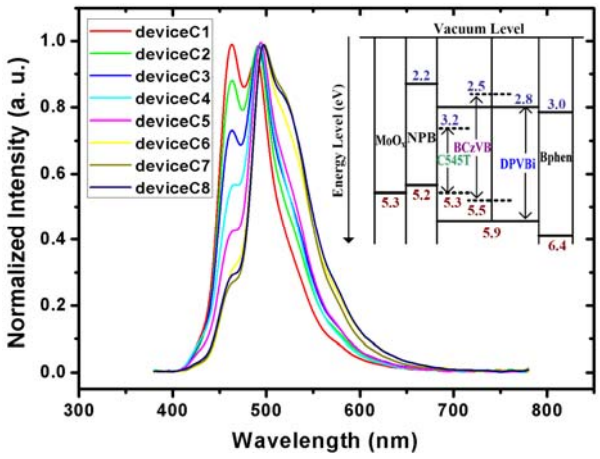

Fig. 7. Normalized EL spectra of Type-C devices at the current density of 20 mA/cm^2. The inset shows the energy diagram of the BOLEDs with a double-EML composed of EML2/EML1.

Table 3. Characteristics of Type-C devices. C545T, L, V, η_L, η_p and CIE (x, y) were the C545T doping concentration, luminance, driving voltage, current efficiency, power efficiency and CIE color coordinates were at 20 mA/cm^2, respectively; the values inside the brackets were the maximum.

Devices	C545T (wt %)	L (cd/m^2)	V (V)	η_L (cd/A)	η_p (Lm/W)	CIE (x, y)
Device C1	0.025	683 (11 748,13[a])	7.8	3.97 (4.25)	1.46 (2.21)	(0.155, 0.244)
Device C2	0.050	762 (12 434,13[a])	8.3	3.82 (4.48)	1.41 (2.34)	(0.168, 0.289)
Device C3	0.075	749 (10 440,14[a])	8.7	3.61 (4.10)	1.38 (2.57)	(0.174, 0.323)
Device C4	0.10	1 174(12 531,14[a])	9.3	3.93 (4.76)	1.27 (2.30)	(0.168, 0.349)
Device C5	0.20	1 081(10 726,15[a])	9.5	3.54 (4.17)	1.16 (2.19)	(0.181, 0.398)
Device C6	0.30	938 (8 657,15[a])	9.6	3.88 (4.36)	1.24 (2.27)	(0.223, 0.482)
Device C7	0.40	784 (10 302,16[a])	9.9	3.49 (4.05)	1.12 (1.81)	(0.211, 0.497)
Device C8	0.80	485 (8 196,17[a])	10.7	3.26 (3.94)	0.89 (1.77)	(0.224, 0.489)

Note:

[a] the driving voltage corresponding to the maximum brightness.

Fig. 8(a)-(c) show the I-V-L characteristics and EL efficiency for Type-C devices. It can be seen that the I–V curve of Type-C devices shifts to lower voltage, indicating the enhancement of hole injections. However, Type-C devices show a lower luminance and current efficiency than that of Type-B devices. The lower efficiency can be understood by a charge imbalance and detrimental exciton quenching processes such as the singlet/triplet–triplet annihilation, the singlet/triplet-polaron quenching and electric field induced dissociation of excitons which occur in the heavily doped OLEDs [20, 21]. In Type-B devices, the 10-nm thick [DPVBi: BCzVB] interlayer was introduced not only to emit but also limit singlet-exciton quenching and reduce holes overflow. This shows that the ability to fine tune the charge transport by double-EML structure with an appropriate sequence is a useful tool for making balanced and efficient devices.

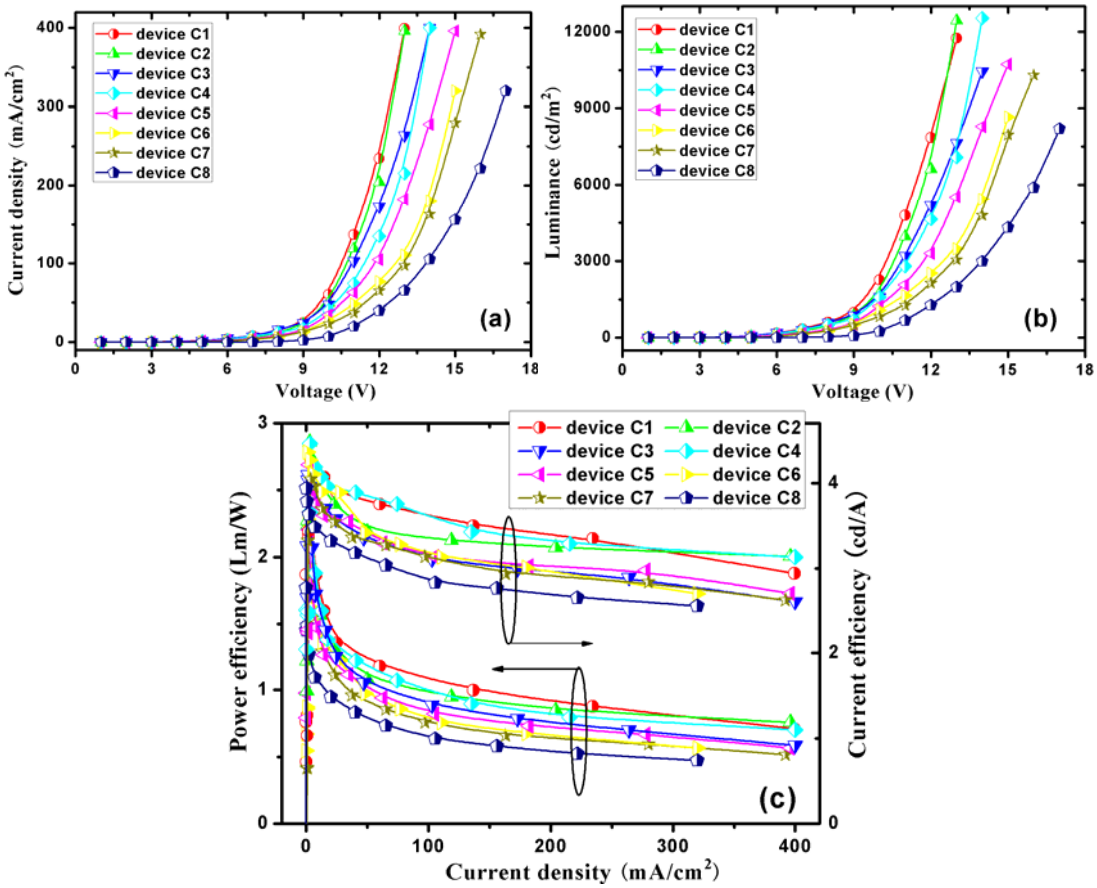

Fig. 8. (a) Voltage–current density (b) luminance–voltage and (c) EL efficiency–current density curves of Type-C devices

4. Conclusion

This paper presents three kinds of BOLEDs, which is fabricated by doping two dopants in one blue host and using the double-EML structures. We first fabricated single-EML BOLEDs based on a double-dopant system. In this BOLED, the emission from C545T was strengthened due to another dopant of BCzVB. Using this double-dopant, the BOLEDs show higher current efficiency as compared to the device without the dopant of C545T. The enhancement of efficiency could readily be realized with an appropriate selection of a matching dopant for efficient energy transfer. Furthermore, we fabricated double-EML BOLEDs following the double-doped structure. We have observed that the double-EML BOLEDs show a striking improvement in chromaticity and current efficiency as compared to the corresponding single-EML counterpart. It is well known that the injection current is very sensitive to the barrier height, and the device efficiency is mainly determined by the number of minority carriers (electrons in this study). Since DPVBi possesses a deep HOMO level of 5.9 eV. It is expected to behave as an effective trapping site for holes. Hence, the d-EML structure with an appropriate stacking sequence easily promotes the balance of carriers in the EML and thereby improving the EL performances.

Acknowledgements

This work is supported by the National Natural Science Foundation of China (60777018, and 60776040), 863 project (2008AA03A336), Shanghai Science and Technology Committee (06DZ22013), and Shanghai Leading Academic Disciplines (S30107).

References

[1] C. W. Tang, S. A. VanSlyke, Applied Physics Letters **51**, 913 (1987)
[2] S. Reineke, F. Lindner, G. Schwartz, N. Seidler, K. Walzer, B. Lüssem, K. Leo, Nature. **459**, 234 (2009).
[3] Kiran T. Kamtekar, Andrew P. Monkman, Martin R. Bryce, Advanced Materials **22**, 572 (2010).
[4] Q. J. Qi, X. M. Wu, Y. L. Hua, Q. C. Hou, M. S. Dong, Z. Y. Mao, B. Yin, S. G. Yin, Organic Electronics **11**, 503 (2010).
[5] J. Lee, J-I. Lee, H.Y. Chu, Synthetic Metals **159**, 1460 (2009).
[6] J. Lee, J.-I. Lee, K.-I. Song, S.J. Lee, H.Y. Chu, Applied Physics Letters **92**, 133304 (2008).
[7] K. S. Kim, Y. M. Jeon, J. W. Kim, C. W. Lee, M. S. Gong, Dyes and Pigments. **77**, 238 (2008).
[8] A. P. Kulkarni, S. A. Jenekhe, Journal of Physical Chemistry **112**, 5174 (2008).
[9] F. S. Li, Z. J. Chen, W. Wei, H. Y. Cao, Q. H. Gong, F. Teng, L. Qian, Y.M. Wang, Journal of Physics D: Applied Physics **37**, 1613 (2004).
[10] H. K. Kim, S. H. Cho, J. R. Oh, Y. H. Lee, J. H. Lee, J.G. Lee, S.K. Ki, Y.I. Park, J.W. Park, Y.R. Do, Organic Electronics **11**, 137 (2010).
[11] Q. Wang, Z.Q. Deng, J.S. Chen , D.G. Ma, Optics Letters **35**, 462 (2010).
[12] J.H. Lee, C.L. Huang, C.H. Hsiao, M.K. Leung, C.C.Yang, C.C. Chao, Applied Physics Letters **94,** 223301 (2009).
[13] S.Y. Seo, J.T. Woo, J.H. Leem, S.H. Lee, M.Jung, D.C. Choo, H.S. Bang, T.W. Kim, S. J. Lee, J.H. Seo, Y.K. Kim, Molecular Crystals and Liquid Crystals **514**, 452 (2009).
[14] W.B. Chen, L.L. Lu, J.B. Cheng, Optik. **121**, 107 (2010).
[15] S.F. Chen, X. Li, W.F. Xie, Y. Zhao, C.A. Li, S.Y. Liu, Thin Solid Films. **516**, 3364 (2008).
[16] K.U. Haq, S.P. Liu , M.A. Khan, X.Y. Jiang, Z.L. Zhang, W. Q. Zhu, Semiconductor Science and Technology **23**, 035024 (2008).
[17] Z.Q. Zhang, Q. Wang, Y.F. Dai, Y.P. Liu, L.X. Wang , D.G. Ma, Organic Electronics **10**, 491 (2009).
[18] X.Y. Zheng, W.Q. Zhu, Y.Z. Wu, X.Y. Jiang, R.G. Sun, Z.L. Zhang, S.H. Xu, Displays. **24**, 121 (2003).
[19] Z.Y. Chen, D.G. Ma, Journal of Luminescence **122–123**, 633 (2007).
[20] S. Reineke, K.Walzer, K. Leo, Physical Review B **75,** 125328 (2007).
[21] J. Lee, J.I. Lee, J.Y. Lee, H.Y. Chu, Synthetic Metals **159**, 1956 (2009).

*Corresponding author: huapinglin@yahoo.com